

# Long-range quantum gates using dipolar crystals

Hendrik Weimer,<sup>1,2,\*</sup> Norman Y. Yao,<sup>1</sup> Chris R. Laumann,<sup>1,2</sup> and Mikhail D. Lukin<sup>1</sup>

<sup>1</sup>*Physics Department, Harvard University, 17 Oxford Street, Cambridge, MA 02138, USA*

<sup>2</sup>*ITAMP, Harvard-Smithsonian Center for Astrophysics, 60 Garden Street, Cambridge, MA 02138, USA*

(Dated: October 14, 2018)

We propose the use of dipolar spin chains to enable long-range quantum logic between distant qubits. In our approach, an effective interaction between remote qubits is achieved by adiabatically following the ground state of the dipolar chain across the paramagnet to crystal phase transition. We demonstrate that the proposed quantum gate is particularly robust against disorder and derive scaling relations, showing that high-fidelity qubit coupling is possible in the presence of realistic imperfections. Possible experimental implementations in systems ranging from ultracold Rydberg atoms to arrays of Nitrogen-Vacancy defect centers in diamond are discussed.

PACS numbers: 03.67.-a, 05.30.Rt, 76.30.Mi, 32.80.Ee

The ability to carry out quantum gates between spatially remote qubits forms a crucial component of quantum information processing [1]. Theoretical and experimental work addressing this challenge has largely been focused upon using photons [2–4], spin chains [5–8] and other hybrid systems [9–11] as quantum buses, which mediate long-range quantum information transfer. In these approaches, this transfer is achieved by either encoding the information in a traveling wavepacket [2–7], or by coupling the remote qubits to a shared spatially extended mode [8–11]. In this Letter, we propose a novel approach to this outstanding problem and demonstrate that adiabatic driving of a dipolar spin system across a quantum phase transition can be used to implement a robust controlled-phase (CP) gate.

Our approach is applicable to dipolar spin systems [12–17], composed, for example, of ultracold atoms and molecules, or solid-state spin ensembles, where natural imperfections invariably lead to disorder. E.g., for spin qubits associated with Nitrogen-Vacancy (NV) centers in diamond [18, 19], the need for both long-range and disorder-robust quantum gates is especially evident. Despite room temperature coherence times of  $\sim 10$  ms, the weakness of magnetic dipole-dipole interactions limits NV spacing to  $\sim 10$  nm for effective two-qubit gates. Even recently demonstrated sub-wavelength techniques [20] cannot address individual NV qubits at such small separations. Moreover, any solid-state quantum bus designed to mediate longer ranged interactions will suffer from positional disorder due to the difficulty of precise nanoscale implantation.

Here, we explore a possible solution to creating a quantum bus within a disordered system. The key element underlying our proposal is a phenomenon discussed in the context of Rydberg atoms as the blockade effect [21–24]. The simultaneous driving of two excitations within length scales shorter than the blockade radius is forbidden as strong interactions shift the doubly-excited state away from resonance. Hence, within the blockade radius, the underlying spatial distribution of the sites is largely ir-

relevant and the arising many-body ground state washes over the effects of disorder and can lead to the formation of crystalline structures [13].

The dynamic crystal formation [13–16] underlying our protocol is schematically illustrated in Fig. 1. We consider two qubits  $A$  and  $B$ , coupled to the ends of a one-dimensional (1D) quantum bus of two state atoms with one electronic ground state and one Rydberg state. The quantum bus is initially prepared in its ground state, containing no Rydberg excitations. Then, the bus is adiabatically driven into the crystal regime. The resulting many-body state has an energy which depends on the boundary conditions set by the state of the qubits. Intuitively, this dependence results from a compression of the crystal, and hence, a decrease in the distance between two Rydberg excitations,  $a_R$ , when the boundary qubits are not excited. Under free evolution, this energy difference is translated into a phase difference, which entangles the qubits. After reversing the adiabatic step, the quantum bus returns to its initial state while the qubits remain entangled.

To be specific, we consider an ensemble of strongly interacting two-state systems described by the Hamiltonian

$$H = -\frac{\hbar\Delta}{2} \sum_i \sigma_i^z + \frac{\hbar\Omega}{2} \sum_i \sigma_i^x + \sum_{i<j} \frac{C_p}{|\mathbf{r}_i - \mathbf{r}_j|^p} P_i^\dagger P_j^\dagger, \quad (1)$$

where  $\Delta$  represents the detuning,  $\Omega$  is the Rabi frequency and  $p = 3$  for dipolar interactions or  $p = 6$  for van der Waals interactions. The interaction strength is characterized by the coefficient  $C_p$  and involve projectors onto one of the states,  $P_i^\dagger = |\uparrow\chi\uparrow\rangle = (1 + \sigma_i^z)/2$ . As we will discuss further below, the same Hamiltonian also applies to NV centers under appropriate driving. Here, the electronic ground state is a spin triplet; thus, the  $m_s = 0$  state corresponds to the atomic ground state, while the  $m_s = 1$  state, which possesses a magnetic dipole moment, corresponds to the excited Rydberg state [18, 19, 25, 26].

An analogous Hamiltonian governs the interactions be-

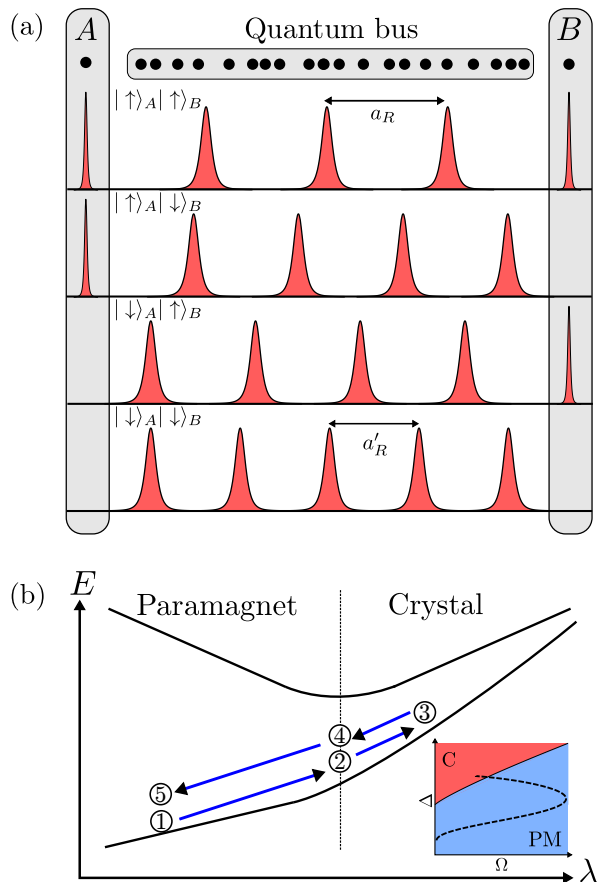


FIG. 1: Setup for the proposed gate. (a) Depending on the state of the qubits  $A$  and  $B$ , the quantum bus (atoms shown as black dots) in the crystalline phase will possess a different ground state, where the distance between two excitations  $a_R$  is altered. This intuitively corresponds to a boundary-condition-dependent compression of the crystal ( $a'_R < a_R$ ). (b) Ground state and first excited state during the control sequence. Initially, the quantum bus is prepared in the paramagnet (1). Then, the control parameter  $\lambda$  is increased adiabatically (2), driving the system across the phase transition. Once in the crystal the system evolves freely and picks up a phase shift depending on the qubit states (3). After the adiabatic process is reversed (4), the quantum bus is disentangled from the qubits (5). The inset shows the phase diagram of the system, with the dashed line depicting the control profile dependent on the Rabi frequency  $\Omega(t)$  and the detuning  $\Delta(t)$ .

tween the boundary qubits ( $A, B$ ) and the quantum bus,

$$H_{int} = \sum_i \frac{C_p}{|\mathbf{r}_A - \mathbf{r}_i|^p} P_A^\dagger P_i^\dagger + \frac{C_p}{|\mathbf{r}_B - \mathbf{r}_i|^p} P_B^\dagger P_i^\dagger. \quad (2)$$

Since the interaction conserves  $\sigma_A^z$  and  $\sigma_B^z$ , any entangling operation between the qubits will be in the form of a CP gate. We may drive the quantum bus independently of the qubits by ensuring that the resonant splitting of the qubits differs from that of the mediating bus; possible implementations will be discussed later.

To derive general scaling properties, we now consider

a one-dimensional system containing  $N$  two-state spins within length  $L$ . The CP gate protocol consists of an adiabatic ramp from the classical ground state into the crystal regime for time  $t_0$ , hold for phase accumulation for time  $t_\pi$  and reverse ramp (another  $t_0$ ), resulting in a total gate time  $t_g = 2t_0 + t_\pi$ . There are three factors which influence the asymptotic scaling of the fidelity with system size: (i) the strength of the effective interaction  $E_{int}$  at the hold point, (ii) the minimum energy gap  $\Delta_g$  (across ramp and qubit sectors) protecting the adiabatic evolution, and (iii) the strength of external decoherence mechanisms. The interaction energy between the qubits, which governs the timescale of entanglement generation, is

$$E_{int} = E_{\uparrow\uparrow} - E_{\uparrow\downarrow} - E_{\downarrow\uparrow} + E_{\downarrow\downarrow}, \quad (3)$$

where  $E_{\alpha\beta}$  refers to the energy of the many-body state with the qubits in state  $|\alpha\rangle_A|\beta\rangle_B$  (Fig. 1). Within the continuum limit of a classical crystal,  $E_{int} \sim d^2/L$  for  $d \ll a_R$ , where  $d$  is the distance between the qubits and the ends of the quantum bus. Owing to quantum fluctuations, the classical crystal cannot be the true ground state, and the system is rather described in terms of a Luttinger liquid [27, 28]. However, such corrections are important only in the limit of very large system sizes ( $N \sim 10^9$  for typical parameters), where they lead to an algebraic decay of the correlation functions [27].

To analyze the effects of a finite gap and decoherence, we consider the contributions of each to the overall error of the controlled phase gate, assuming they occur independently [29]. While, in the thermodynamic limit, the gap vanishes at the phase transition, here, we consider finite system sizes where there always exists a non-zero gap. For gapless phases such as the dipolar crystal however, it is important to note that the gap may further decrease upon entering the ordered phase. The qualitative effect of such a finite gap is described within a Landau-Zener framework. Optimizing the form of the Landau-Zener sweep by introducing a nonlinearity results in an improved error scaling with,  $\varepsilon_{LZ} = \exp(-c\Delta_G t_0/\hbar)$ , where  $c$  is a model-dependent numerical constant [30, 31]. In the case of the dipolar crystal,  $\Delta_G \sim 1/L$ , due to the phononic nature of the excitations [27, 28]; this results in an error which scales according to the theoretical optimum given by the Lieb-Robinson bound for the speed of information transfer [32].

Next, we consider the effects of decoherence, noting that the induced error is a monotonically increasing function dependent only on the product of the decoherence rate  $\gamma$  and the total gate time  $t_g$ . In particular, we assume,  $\varepsilon_d = 1 - \exp[-(\gamma t_g)^\delta] \approx (\gamma t_g)^\delta$ , where  $\delta$  depends on the physical details of the decoherence process [33]. The highly entangled nature of the various many-body states depicted in Fig. 1 implies that the effective decoherence rate must scale with the system size,  $\gamma = \gamma_0 \frac{L}{L_0}$ , where  $\gamma_0$  is the single particle decoherence rate and the length scale

$L_0$ . In the dipolar crystal,  $L_0$  is approximately given by the average distance between two excited spins; this is consistent with intuition, as decoherence processes ought only be relevant at sites where there exists an actual excitation.

To separate off the explicit system size dependence within  $\varepsilon_{LZ}$ , we define  $\alpha_0 = cL\Delta_G/\hbar$ . Combining the two error contributions and conservatively plugging  $t_g > t_0$  into the form for  $\varepsilon_{LZ}$ , then yields

$$\varepsilon_T = \exp\left(-\frac{\alpha_0}{L}t_g\right) + \left(\gamma_0\frac{L}{L_0}t_g\right)^\delta. \quad (4)$$

By minimizing the total error, we obtain an optimal gate time,  $t_g^{\text{opt}} = \delta L \log[L_0\alpha_0/(L^2\gamma_0)]/\alpha_0$ , with corresponding error,

$$\varepsilon_T = L^{2\delta} \left( \delta \frac{\gamma_0}{L_0\alpha_0} \log \frac{L_0\alpha_0}{L^2\gamma_0} \right)^\delta. \quad (5)$$

Thus, our protocol exhibits a scaling analogous to a quantum gate based on a microscopic interaction with energy  $C_2/L^2$ , which has an error given by  $\varepsilon = L^{2\delta}(2\pi\gamma_0/C_2)^\delta$ . The precise values of  $\alpha_0$  and  $L_0$  can be derived from numerical studies, as we will show in the following.

*Simulations.* — In these numerical simulations, we both verify our general scaling arguments and demonstrate the ability to achieve superior gate fidelities in comparison to bare microscopic interactions. We begin by considering a chain of  $N$  equidistant or uniformly randomly distributed particles with average interparticle spacing  $a$ ; the details of the numerical simulation method are described in [13]. Initially, the qubits are prepared in the state  $|\psi\rangle_{A,B} = (|\uparrow\rangle_A + |\downarrow\rangle_A) \otimes (|\uparrow\rangle_B + |\downarrow\rangle_B)/2$ , while the spin chain is fully polarized,  $|\psi\rangle_{SC} = \prod_i |\downarrow\rangle_i$ . This initial qubit state constitutes a worst-case scenario leading to a minimum value of the fidelity for relevant decoherence models, including pure dephasing. Using a different initial state for the qubits can lead to a significantly higher fidelity. To drive the system across its phase transition, external control fields are then varied according to

$$\Omega(t) = \Omega_0 \sin^2\left(\frac{8t/t_0}{1 + 16t^2/t_0^2}\right) \quad (6)$$

$$\Delta(t) = \Delta_0[1 - 5\exp(-4t/t_0)]. \quad (7)$$

Here,  $\Omega_0$  is chosen such that the endpoint of the ramp lies just within the crystalline phase, see Fig. 1. While the proposed ramp profile features the requisite nonlinearity, its details have yet to be optimized; therefore, with optimal control theory, it may be possible to further enhance the achievable gate fidelities [34]. At  $t = t_0$ , the system freely evolves for a time,  $t_\pi = \pi\hbar/E_{\text{int}}$ , in order to allow the effective interaction to generate a phase gate between the qubits. Following this period of free evolution, the adiabatic ramp is then reversed. In addition to naturally following the reversed profile, an alternate implementation can also be achieved by a complete

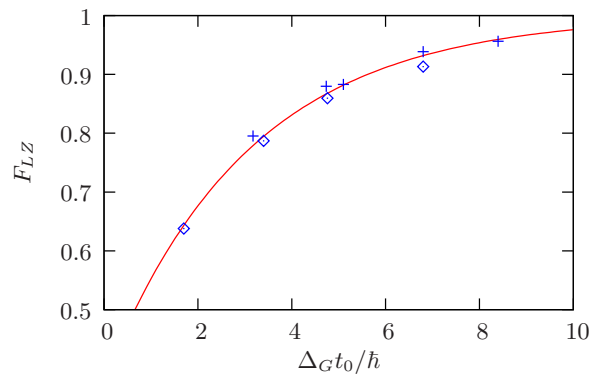


FIG. 2: Numerical simulation results for the gate fidelity  $F_{LZ}$  due to non-adiabatic transitions depending on the product of the gap  $\Delta_G$  and duration of the adiabatic step  $t_0$  for equidistant ( $N = 34$ , diamonds) and disordered ( $N = 15$ , crosses) configurations. The gap has been varied by changing  $\Omega_0$  while all other parameters are held fixed. The solid line is an exponential fit to the data. ( $p = 3$ ,  $C_3 = 100 \hbar\Omega_0 a^3$ ,  $\Delta_0 = 2.3 \Omega_0$ ,  $d = 3a$ ).

reversal of Hamiltonian dynamics upon switching  $H$  to  $-H$ . The ability to change the sign of the interaction depends on the physical implementation; in the case of Rydberg atoms, this can be achieved by transferring the population from a repulsive state to an attractive state or by changing an external electric field [35]. We find that both protocols give nearly identical results and focus on the latter, as it simplifies the numerical analysis. Since our procedure implements a controlled phase gate up to local rotations, the fidelity of the proposed gate is then given by the disentanglement fidelity between the qubits and the chain,  $F_{LZ} = \sqrt{\text{Tr}\{\rho_{AB}^2\}}$ , where  $\rho_{AB}$  is the qubits' reduced density matrix.

In the absence of decoherence, we expect the errors to be characterized by a Landau-Zener exponential and this is indeed revealed by the simulations, as shown in Fig. 2; the fidelity is well-characterized by  $F = 1 - b\exp(-c\Delta_G t_0/\hbar)$ , where  $b$  and  $c$  are numerical fit parameters. Combining these numerics with the additional errors associated with decoherence ( $\varepsilon_d$ ) yields an overall fidelity,

$$F_T = \frac{1}{2} [1 - b e^{-c\Delta_G t_0/\hbar}] \left[ 1 + e^{-\left(\gamma_0 \frac{L}{t_0} \left[ 2t_0 + \frac{\pi\hbar}{E_{\text{int}}} \right] \right)^\delta} \right]. \quad (8)$$

Note that for near-perfect gates this expression is equivalent to Eq. (4). As previously discussed, there now exists a maximum fidelity, which is achieved by an optimal ramp time,  $t_0$  that is a function of only the effective interaction strength,  $E_{\text{int}}$ , and the gap,  $\Delta_G$ .

Crucially, Eq. (8) now allows us to investigate the consequences of a disordered interparticle spacing. For a 1D dipolar crystal, it is known that the crystal spacing,  $a_R = [\zeta(p)(p+1)C_p/\Delta]^{1/p}$ , is essentially independent of the spacing between individual particles, suggesting that

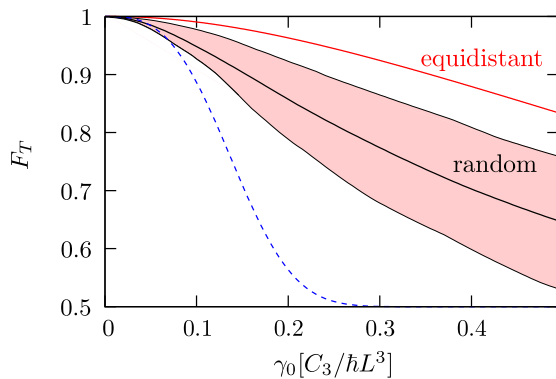


FIG. 3: Dependence of the maximum fidelity of the proposed quantum gate on the single particle decoherence rate  $\gamma_0$  with parameters taken from the numerical simulation for a system size of  $L$  and a spin-echo suppressed decoherence rate with  $\delta \approx 3$ . The solid red line is the fidelity in the equidistant case with  $N = 34$  particles, while the shaded areas correspond to 90% confidence intervals for a disordered situation ( $N = 51$ ). The dashed line indicates the fidelity that can be achieved using the bare dipolar interaction between the qubits.

the crystalline phase may be robust against effects of disorder [27]. To evaluate the gate fidelity (8), we numerically determine the gap,  $\Delta_G$ , and the interaction energy,  $E_{\text{int}}$ , for 100 different uniformly distributed random configurations for the parameters as in Fig. 2 ( $b = 0.62$ ,  $c = 0.32$ ). By extracting  $L_0 = L / \sum_i \langle P_i^\dagger \rangle = 2.0 (C_3/\Omega_0)^{1/3}$  from the average density of excitations and employing Eq. (8), we then calculate the optimum adiabatic ramp time  $t_0$  and hence, the maximum gate fidelity. The result is shown in Fig. 3. Significantly, *even* in the presence of disorder, the fidelity of our phase gate is higher than that which can be achieved via microscopic dipolar interactions.

*Experimental Realization.*— In the case of Rydberg atoms, it is possible to achieve independent addressing of the boundary qubits by choosing differing hyperfine levels for the qubit and quantum bus atoms. Our proposed protocol can be realized through either van der Waals interactions ( $p = 6$ ) between  $S$  states or through dipolar interactions ( $p = 3$ ) between states within an electric-field induced Stark fan [36]. Let us focus on the latter case and consider a Rydberg state with principle quantum number  $n = 43$  and decoherence rate  $\gamma_0 = 10$  kHz ( $\delta = 1$ ), neglecting the effects of atomic motion, which is well justified at temperatures on the order of 100 nK. In order to achieve a gate fidelity,  $F = 0.9$ , the requisite laser parameters are given by  $\Omega_0 = 2\pi \times 8$  MHz,  $\Delta_0 = 2\pi \times 17$  MHz, and the corresponding interaction strength is given by  $C_3 a^{-3} = 2\pi \times 800$  MHz. Such an interaction strength can be achieved in a Rydberg atom cloud with an average interparticle spacing of  $a \approx 1\mu\text{m}$ , leading to  $L \approx 40\mu\text{m}$ ; we note that these parameters are compatible with present experimental techniques [37].

For van der Waals interactions, the enhancement of the phase gate fidelity is even more pronounced.

It is also possible to implement our protocol using a solid-state room temperature setup based upon NV defect centers in diamond [18, 19]. To realize the Hamiltonian (1) using a quasi-1D chain of NV centers [38–40], we work with the  $m_s = 0, 1$  electronic spin states with crystal field splitting  $\approx 2.8$  GHz. Independent addressing of the qubits and quantum bus can be achieved by using a different Nitrogen isotope ( $^{15}\text{N}$ ) for the qubits and the bus ( $^{14}\text{N}$ ); the hyperfine coupling between the NV electronic spin and the Nitrogen nuclear spin is isotope dependent, with  $A_{\parallel}^{N15} \approx 3.03$  MHz and  $A_{\parallel}^{N14} \approx -2.14$  MHz [41]. This difference ensures that the microwave driving of the quantum bus is off-resonant with the qubit splitting, allowing for independent initialization and control. Alternatively, the boundary qubits may be taken as bare Nitrogen impurities manipulated by a nearby NV center. The Nitrogen electron spin functions as the boundary spin for the protocol and features resonance frequencies detuned by GHz, which potentially allows for stronger driving during the gate procedure.

While recent experiments have demonstrated optical initialization of the  $m_s = 0$  state with approximately 92–95% fidelity, it may be possible to further enhance this initialization by exploiting the neutral  $\text{NV}^0$  charge state. In particular, recent work [42] has shown that red laser excitation can transfer nearly 100% of the population to one  $m_s$  sublevel of the spin-1/2  $\text{NV}^0$  electronic spin. This enables us to effectively polarize the NV nuclear spins of the chain via cycles of microwave and red laser driving. Finally, after returning the defect to the  $\text{NV}^-$  charge state, a SWAP gate transfers the polarization from the nuclear spins back to the spin-1 electronic spins of the  $\text{NV}^-$ . Such enhanced initialization may prove beneficial for other NV-based quantum computing architectures [26].

Magnetic field fluctuations (e.g., from a nuclear spin bath), which give rise to  $T_2^*$  dephasing processes can effectively be suppressed by stroboscopically switching the system between the  $m_s = \pm 1$  states. In the resulting dynamics, the electronic spin is then decoupled from the environment and coherence times up to the spin relaxation time  $T_1$  can be achieved [43]. This procedure also leads to the suppression of undesired flip-flop couplings between the NV centers. Assuming  $\gamma_0 = 100$  Hz [44], a Rabi frequency  $\Omega_0 = 2\pi \times 62$  kHz, a detuning  $\Delta_0 = 2\pi \times 130$  kHz, and an average NV spacing of  $a = 2$  nm, according to the results shown in Fig. 3, we can achieve gate times  $t_g \approx 500\mu\text{s}$  and fidelities of  $F = 0.98$  in the equidistant case, and  $F = 0.93 \pm 0.04$  for disordered configurations over a distance of  $L = 74$  nm. We stress that such qubit distances are compatible with the individual optical addressing and readout of NV qubits using experimentally demonstrated sub-wavelength techniques [20, 45].

In summary, we have shown that a robust long-range

quantum gate can be created using dipolar spin chains. We have discussed possible experimental realizations with Rydberg atoms or NV centers and emphasize that the proposed long-range gate can tolerate disorder. At the same time, the proposed gate is not limited to the case of dipolar crystals; indeed, one can implement our protocol within the transverse Ising model, wherein even a nearest-neighbor interaction can be used to create an effective  $1/L^2$  power law interaction. Finally, our proposal is also a first step towards studying quantum many-body physics with NV centers.

We acknowledge fruitful discussions with P. Zoller, L. Huijse, and A. Chandran. This work was supported by the National Science Foundation through a grant for the Institute for Theoretical Atomic, Molecular and Optical Physics at Harvard University and Smithsonian Astrophysical Observatory, a fellowship within the Postdoc Program of the German Academic Exchange Service (DAAD), the DOE (FG02-97ER25308), the Lawrence Golub Fellowship, CUA, NSF, DARPA, AFOSR MURI, and the Packard Foundation.

---

\* Electronic address: hweimer@cfa.harvard.edu

- [1] D. P. DiVincenzo, *Fortschr. Phys.* **48**, 771 (2000).
- [2] J. I. Cirac et al., *Phys. Rev. Lett.* **78**, 3221 (1997).
- [3] D. L. Moehring et al., *Nature (London)* **449**, 68 (2007).
- [4] E. Togan et al., *Nature* **466**, 730 (2010).
- [5] S. Bose, *Phys. Rev. Lett.* **91**, 207901 (2003).
- [6] M. Christandl et al., *Phys. Rev. Lett.* **92**, 187902 (2004).
- [7] G. Gualdi et al., *Phys. Rev. A* **78**, 022325 (2008).
- [8] N. Y. Yao et al., *Phys. Rev. Lett.* **106**, 040505 (2011).
- [9] N. J. Craig et al., *Science* **304**, 565 (2004).
- [10] Y. Rikitake and H. Imamura, *Phys. Rev. B* **72**, 033308 (2005).
- [11] P. Rabl et al., *Nature Phys.* **6**, 602 (2010).
- [12] P. Rabl and P. Zoller, *Phys. Rev. A* **76**, 042308 (2007).
- [13] H. Weimer et al., *Phys. Rev. Lett.* **101**, 250601 (2008).
- [14] T. Pohl, E. Demler, and M. D. Lukin, *Phys. Rev. Lett.* **104**, 043002 (2010).
- [15] J. Schachenmayer et al., *New J. Phys* **12**, 103044 (2010).
- [16] R. M. W. van Bijnen et al., *J. Phys. B* **44**, 184008 (2011).
- [17] A. V. Gorshkov et al., *Phys. Rev. Lett.* **107**, 115301 (2011).
- [18] L. Childress et al., *Science* **314**, 281 (2006).
- [19] M. V. G. Dutt et al., *Science* **316**, 1312 (2007).
- [20] P. C. Maurer et al., *Nature Phys.* **6**, 912 (2010).
- [21] D. Jaksch et al., *Phys. Rev. Lett.* **85**, 2208 (2000).
- [22] M. D. Lukin et al., *Phys. Rev. Lett.* **87**, 037901 (2001).
- [23] E. Urban et al., *Nature Phys.* **5**, 110 (2009).
- [24] A. Gaëtan et al., *Nature Phys.* **5**, 115 (2009).
- [25] P. Neumann et al., *Nature Phys.* **6**, 249 (2010).
- [26] N. Y. Yao et al., arXiv:1012.2864 (2010).
- [27] H. Weimer and H. P. Büchler, *Phys. Rev. Lett.* **105**, 230403 (2010).
- [28] E. Sela, M. Punk, and M. Garst, *Phys. Rev. B* **84**, 085434 (2011).
- [29] X. Lacour et al., *Phys. Rev. A* **75**, 033417 (2007).
- [30] J. Roland and N. J. Cerf, *Phys. Rev. A* **65**, 042308 (2002).
- [31] H. T. Quan and W. H. Zurek, *New J. Phys.* **12**, 093025 (2010).
- [32] E. H. Lieb and D. W. Robinson, *Commun. Math. Phys.* **28**, 251 (1972).
- [33] J. R. Maze, J. M. Taylor, and M. D. Lukin, *Phys. Rev. B* **78**, 094303 (2008).
- [34] N. Khaneja, R. Brockett, and S. J. Glaser, *Phys. Rev. A* **63**, 032308 (2001).
- [35] T. J. Carroll et al., *Phys. Rev. Lett.* **93**, 153001 (2004).
- [36] G. Pupillo et al., *Phys. Rev. Lett.* **104**, 223002 (2010).
- [37] M. Saffman, T. G. Walker, and K. Mølmer, *Rev. Mod. Phys.* **82**, 2313 (2010).
- [38] D. M. Toyli et al., *Nano Lett.* **10**, 3168 (2010).
- [39] P. Spinicelli et al., *New J. Phys.* **13**, 025014 (2011).
- [40] B. J. M. Hausmann et al., *New J. Phys.* **13**, 045004 (2011).
- [41] S. Felton et al., *Phys. Rev. B* **79**, 075203 (2009).
- [42] G. Waldherr et al., *Phys. Rev. Lett.* **106**, 157601 (2011).
- [43] G. de Lange et al., *Science* **330**, 60 (2010).
- [44] G. Balasubramanian et al., *Nature Mater.* **8**, 383 (2009).
- [45] E. Rittweger et al., *Nature Photon.* **3**, 144 (2009).